Journal of Applied Polymer Science

Influence of rubber content on mechanical, thermal, and morphological behavior of natural rubber toughened poly(lactic acid)-multiwalled carbon nanotube nanocomposites

Mohd Shaiful Zaidi Mat Desa,[1,2] Azman Hassan,[1] Agus Arsad,[1] Reza Arjmandi,[1] Nor Nisa Balqis Mohammad[1]

[1]Enhanced Polymer Research Group, Department of Bioprocess and Polymer Engineering, Faculty of Chemical Engineering, Universiti Teknologi Malaysia, 81310 UTM Skudai Johor, Malaysia

[2]Faculty of Chemical & Natural Resources Engineering, Universiti Malaysia Pahang, Lebuhraya Tun Razak, 26300 Gambang Kuantan, Malaysia

Correspondence to: A. Arsad (E-mail: agus@cheme.utm.my)

ABSTRACT: The effects of natural rubber (NR) on the mechanical, thermal, and morphological properties of multiwalled carbon nanotube (CNT) reinforced poly(lactic acid) (PLA) nanocomposites prepared by melt blending were investigated. A PLA/NR blend and PLA/CNT nanocomposites were also produced for comparison. The tensile strength and Young's modulus of PLA/CNT nanocomposites improved significantly, whereas the impact strength decreased compared to neat PLA. The incorporation of NR into PLA/CNT significantly improved the impact strength and elongation at break of the nanocomposites, which showed approximately 200% and 850% increases at 20 wt % NR, respectively. However, the tensile strength and Young's modulus of PLA/NR/CNT nanocomposites decreased compared to PLA/CNT nanocomposites. The morphology analysis showed the homogeneous dispersion of NR particles in PLA/NR/CNT nanocomposites, while CNTs preferentially reside in the NR phase rather than the PLA matrix. In addition, the incorporation of NR into PLA/CNT lowered the thermal stability and glass-transition temperature of the nanocomposites.
 J. Appl. Polym. Sci. **2016**, *133*, 44344.

KEYWORDS: biopolymers & renewable polymers; graphene and fullerenes; mechanical properties; nanotubes; rubber; thermal properties

Received 20 October 2015; accepted 10 August 2016
DOI: 10.1002/app.44344

INTRODUCTION

Nonbiodegradable plastic wastes have caused serious environmental pollution problems. Therefore, there is a strong research interest in the development of biodegradable polymeric materials from renewable resources in order to reduce plastics waste pollution and the consumption of petroleum-based polymers.[1] Among the commercially available biobased polymers, poly(lactic acid) (PLA) is one of the most widely explored in recent years.[1–5] PLA is an aliphatic polyester produced by polymerization of lactic acid, which can be obtained from fermentation of agricultural residue such as corn starch.[3] Rapid progress in research and development has enabled large-scale production of PLA with good mechanical properties comparable to commercial polymers such as poly (ethylene terephthalate) (PET).[2,6] Although PLA possesses good tensile strength and elastic modulus, the elongation at break and impact strength are relatively poor. This brittle characteristic of PLA is considered to be the main drawback that limits its application in areas that require high toughness.[2,4,5]

To further enhance the mechanical strength of PLA, one of the most promising strategies is through the incorporation of nanofillers such as carbon nanotubes (CNT),[7–12] graphene,[13] montmorillonite,[14,15] and halloysite nanotubes[16] to form polymer nanocomposites. PLA/CNT nanocomposites have attracted strong research interest because of the ability of CNT to impart good mechanical, thermal, and electrical properties.[7–12] Processing and preparation are the most crucial elements in PLA/CNT nanocomposite development, since they will affect the dispersion and interfacial interaction properties of the polymer blend. Researchers have adopted solution-mixing[7,17,18] and melt-blending[8,19,20] techniques to achieve better dispersion of CNTs in a PLA matrix. Moreover, functionalization of CNTs is also shown to enhance the dispersion of CNTs in the PLA matrix.[9] However, despite the improvement of tensile strength and stiffness, the incorporation of CNTs is shown to reduce the impact strength and elongation at break of PLA.[7,11,12] Therefore, further investigations on the toughening of PLA/CNT nanocomposites are needed to realize the true potential of PLA for wider applications.

The improvement of toughness in PLA and its nanocomposites can be achieved by blending with plasticizers, elastomers, and other ductile polymers. For instance, the use of plasticizers is shown to effectively enhance the toughness of PLA, whereas the thermal stability of the blend decreased due to reduction of the glass-transition temperature (T_g).[21] The ductile polymers such as linear low-density polyethylene, poly(ε-caprolactone), and ethylene vinyl-*co*-acetate (EVA) were reported to improve the toughness of PLA.[22–25] More recently, natural rubbers (NR) are also reported to improve the toughness of PLA.[26–33] NR, which originates from renewable resources, displays high elasticity, flexibility, and toughness and has been used as a impact modifier to improve the toughness of brittle polymers.[34] In addition, NR can be distributed evenly as small particles in a PLA matrix to enhance the energy absorption, resulting in increased toughness of the system.[31] In a recent study, it was shown that the addition of maleic anhydride (MA) grafted with NR (NR-*g*-MA) into PLA/NR blends led to an improvement in impact strength.[35]

The effect of NR as an impact modifier in PLA nanocomposites has also been reported. Bijarimi *et al.*[36] showed a 143% increase in impact strength with the addition of 10 wt % NR in a PLA/nanoclay nanocomposite compared to neat PLA. In a preliminary study, the mechanical properties of NR-toughened PLA nanocomposite at varying NR contents and 1 phr CNT were investigated.[37] The study revealed that the impact strength increased with increasing NR content in PLA/CNT nanocomposites, with a concomitant decrease in tensile strength and Young's modulus. In addition, the effect of pristine nonfunctionalized multiwalled carbon nanotubes (p-CNT) on the mechanical properties of NR-*g*-MA compatibilized PLA/NR blends (PLA/NR/NR-*g*-MA) at different p-CNT loadings were recently investigated.[38] It was shown that with increasing p-CNT content the Young's modulus increased but the tensile strength and impact strength decreased.

The current study is a more comprehensive one investigating the effects of NR content on the mechanical, thermal, and morphology properties of carboxylic functionalized multiwalled CNT reinforced PLA nanocomposites prepared by a melt-blending technique. The CNT content was fixed at 5 phr based on our previous study,[12] which indicated that the optimum CNT content in PLA/CNT nanocomposites was 5 phr CNT.

EXPERIMENTAL

Materials

Injection-grade poly(lactic acid) (PLA 1323A) was purchased from Shenzen Esun Industrial Co. Ltd., Shenzen, People's Republic of China with 1.35 g/cm^3 density, a melt index of 7 g/10 min (2.16 kg load), and melting temperature of 150 °C. Carboxylic functionalized multiwalled carbon nanotubes with average diameter of 10–11 nm and length of 12–15 µm were obtained from Shandong Dazhan Nano New Material Co. Ltd., Binzhou, People's Republic of China with a purity of greater than 98% produced via chemical vapor deposition (CVD) with 10 atom % of carboxylic acid functional groups. Natural rubber (T_g −70 °C) was supplied by the Malaysia Rubber Board, Kuala Lumpur, Malaysia.

Table I. Polymer Nanocomposite Compositions

	Composition		
Formulations	PLA (wt %)	NR (wt %)	CNT (phr)
PLA	100	0	0
PLA/NR	90	5	0
PLA/CNT	100	0	5
PLA/NR(5)/CNT	95	5	5
PLA/NR(10)/CNT	90	10	5
PLA/NR(15)/CNT	85	15	5
PLA/NR(20)/CNT	80	20	5

Nanocomposites and Blend Preparation

Before the mixing and extrusion process, PLA was dried for 24 h at 40 °C in a vacuum oven to remove moisture. It is known that the hydrolysis of PLA typically accelerates in humid conditions above its glass-transition temperature.[20] Therefore, the drying of PLA is required to avoid hydrolysis degradation of PLA during processing. Raw NR was masticated for 20 min at a temperature below 40 °C and later chopped into small pieces. As pointed out by Jararotkamrjorn *et al.*,[31] the mastication of NR is necessary to reduce the molecular weight and viscosity of NR for better processing and toughening effects.

PLA, NR, and CNT were melt-blended using a counterrotating twin-screw extruder (Brabender Plasticoder PL 200, Duisburg, Germany) having a screw diameter of 19 mm and barrel length of 450 mm ($L/D = 24$) with 40 rpm screw speed, while the mixing temperature was varied between 160 and 190 °C. For PLA/NR(a)/CNT nanocomposite preparation, the content of natural rubbers was varied between 5 and 20 wt %, where (a) denotes the NR loading for each formulation. The content of CNT was kept constant at 5 phr in the nanocomposite formulations. Table I summarizes the compositions of all nanocomposite formulations. All of the extruded samples were pelletized and injection-molded into test specimens for further mechanical analysis. For comparison, sample formulations of neat PLA, a PLA/CNT nanocomposite with 5 phr CNT, and a PLA/NR blend with 5 wt % NR were also prepared.

Mechanical Testing

The effects of different loadings of NR in the PLA matrix nanocomposite on the mechanical properties of the new PLA nanocomposite were evaluated by tensile and impact testing according to ASTM D638 and ASTM D256, respectively, on at least five specimens for each formulation. Tensile tests were performed using a Lloyd testing machine, West Sussex, United Kingdom with a testing speed of 5 mm/min. Flexural tests were also carried out with the Lloyd testing machine with a 3 mm/min testing speed. Impact strength was measured on V-notched specimens with Izod test methods using a Toyoseiki Izod impact tester, Tokyo, Japan. All tests were carried out under ambient conditions.

Morphology Analysis

The impact-fractured surfaces of selected PLA nanocomposite samples were observed using a Carl Zeiss Supra 35 field emission

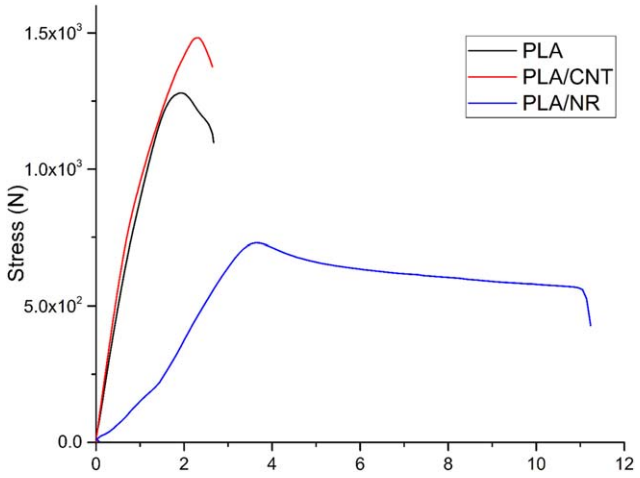

Figure 1. Stress–strain plots of PLA, PLA/NR, and PLA/CNT. [Color figure can be viewed at wileyonlinelibrary.com.]

scanning electron microscope (FESEM, Jena, Germany) with 10 mm working distance and accelerating voltage of 10.00 kV. All samples were coated with a thin layer of gold prior to observation under the electron beam.

The morphology of the PLA/NR/CNT nanocomposites was further investigated with an energy-filtered transmission electron microscope (EFTEM) model Carl Zeiss Libra at 120 kV. Ultrathin sections of the specimens with a thickness of less than 0.1 µm were cut using an RMC Power Tome XL ultramicrotome, Tucson, Arizona, United States of America with a cryodiamond knife. Cut sections were placed on a copper grid for observation under TEM.

Thermal Properties Analysis

The melting and crystallization behaviors of the nanocomposites were studied using a PerkinElmer DSC-6 differential scanning calorimeter (DSC, Waltham, Massachusetts, United States) under nitrogen atmosphere. Prior to this, all samples were weighed at about 10 mg and sealed into aluminum pans. For the first heating scan, the temperature was gradually raised from 30 to 180 °C at 10 °C/min heating rate to eliminate the influence of thermal and mechanical history. After a period of 1 min, the samples were cooled to 30 °C at the same rate. The second heating scan was carried out using a temperature range and heating rate similar to the first heating scan. The glass-transition temperature (T_g), melting temperature (T_m), and degree of crystallinity (X_c) of neat PLA, PLA/NR, PL/CNT, and all NR-toughened PLA/CNT nanocomposites were determined. The degree of crystallinity (X_c) of all specimens was characterized using the following equation:

$$X_c(\%) = \frac{\Delta H_m}{\Delta H_m^o \times \varnothing} \times 100\% \quad (1)$$

where ΔH_m is the fusion enthalpy of PLA measured from the DSC analysis, $\varnothing$ is the weight fraction of PLA in the sample, and ΔH_m^o is the fusion enthalpy of PLA at 100% crystallinity, selected as 93 J/g.[25]

The evaluation of the thermal-degradation behavior was analyzed using thermogravimetric analysis (TGA) in a TA model Q500 thermogravimetric analyzer, New Castle, Delaware, United States of America. Samples of about 12 mg were added to alumina crucibles and heated from 25 to 500 °C at a heating rate of 20 °C/min under nitrogen atmosphere.

RESULTS AND DISCUSSION

Mechanical Properties

Figure 1 illustrates the stress–strain curve of neat PLA, PLA/CNT, and PLA/NR, and Table II shows the comparison of their respective mechanical properties. It is clear that the presence of CNT increased the tensile strength and stiffness of PLA, as revealed by the 29% and 4% increase in tensile strength and Young's modulus, respectively. However, as expected, PLA/CNT displayed lower impact strength than neat PLA due to the presence of rigid CNT nanofillers. On the other hand, Table II also shows an increase in impact strength and elongation at break for PLA/NR blends as compared to neat PLA. This finding shows a promising application of NR to act as an efficient impact modifier for PLA. However, the increase in impact strength was accompanied by a decrease in tensile strength and Young's modulus due to the low modulus of the NR phase.

In general, Figure 2(a) shows that the addition of NR decreased the tensile strength and Young's modulus of PLA/CNT. At 5 wt % of NR, both the tensile strength and Young's modulus of the nanocomposites decreased by 25% compared to the PLA/CNT. Subsequently, Figure 2(a) also shows that a further increase in NR content resulted in a gradual decrease of Young's modulus and tensile strength. This is mainly due to the influence of low-modulus NR and the low crystallinity of PLA in the ternary nanocomposite system.[25,33,39] The decrease in stiffness and tensile strength was also attributed to low dispersion of nanotubes in the PLA matrix of the PLA/NR/CNT nanocomposite system, which will be discussed later in the morphology analysis section.

From Figure 2(b), it can be noted that PLA/NR(5)/CNT showed lower elongation at break than PLA/NR, which demonstrates the decrease in ductility with the presence of CNT. This is expected, due to the high rigidity behavior of CNT. On the other hand, the ductility of the nanocomposites was increased with the incorporation of NR, which was represented by the increasing trend of elongation at break with further increase of NR in

Table II. Mechanical Properties of PLA, PLA/NR, and PLA/CNT

Formulations	Tensile strength (MPa)	Young's modulus (GPa)	Elongation at break (%)	Impact strength (kJ/m^2)
PLA	33.67 ± 1.13	3.24 ± 0.08	2.44 ± 0.25	3.35 ± 0.35
PLA/NR	21.41 ± 1.10	0.89 ± 0.04	11.93 ± 1.68	4.52 ± 0.38
PLA/CNT	43.35 ± 1.43	3.37 ± 0.08	2.44 ± 0.22	1.84 ± 0.14

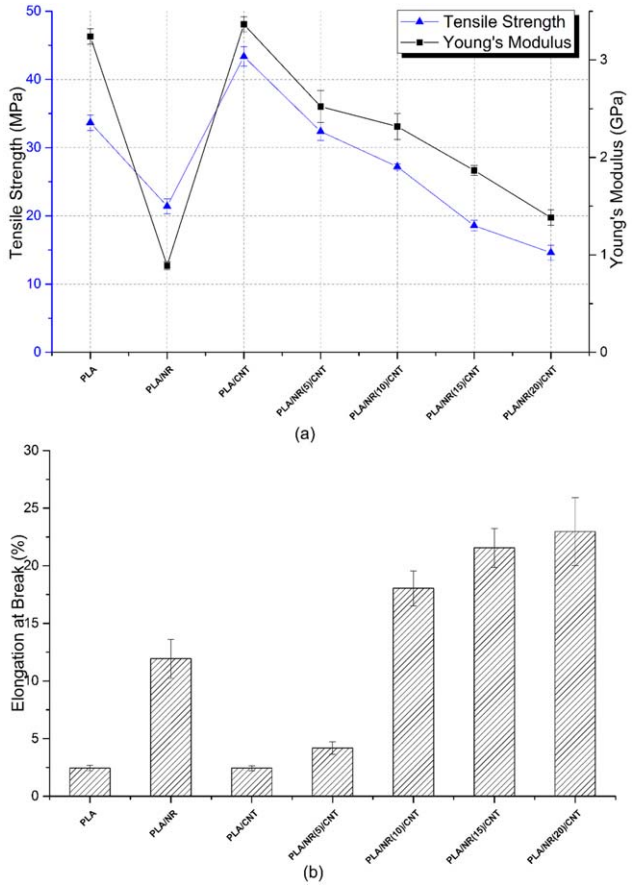

Figure 2. Tensile properties of PLA, PLA/NR, PLA/CNT, and PLA/NR/CNT at various NR contents. [Color figure can be viewed at wileyonlinelibrary.com.]

the nanocomposite systems. By comparing with PLA/CNT, it is interesting to note that after a modest 70% increase of elongation at break in PLA/NR(5)/CNT, a larger increase was observed in PLA/NR(10)/CNT (640% increase), followed by a slight increase in PLA/NR(15)/CNT and PLA/NR(20)/CNT, with 780% and 850% increases, respectively. This observation is presumably related to the optimum size and distribution of rubber particles displayed in the PLA/NR(10)/CNT nanocomposite system, which will be discussed later in the morphology analysis section. Among all the PLA/NR/CNT nanocomposites, PLA/NR(5)/CNT displayed the highest Young's modulus (2.52 GPa) and tensile strength (32.38 MPa), while the highest elongation at break was displayed by PLA/NR(20)/CNT.

As observed in Figure 3, in comparison to the flexural properties of PLA/CNT, the PLA/NR(5)/CNT shows a significant decrease in flexural strength and flexural modulus of 24% and 34%, respectively. Subsequent introduction of more NR into PLA/CNT resulted in a steady decrease in flexural properties. The lowest flexural properties were displayed by PLA/NR(20)/CNT, which recorded 68% and 49% decreased flexural strength and flexural modulus, respectively, compared to PLA/CNT nanocomposites. The decrease in flexural strength and modulus was related to the presence of phase-separated low-modulus NR

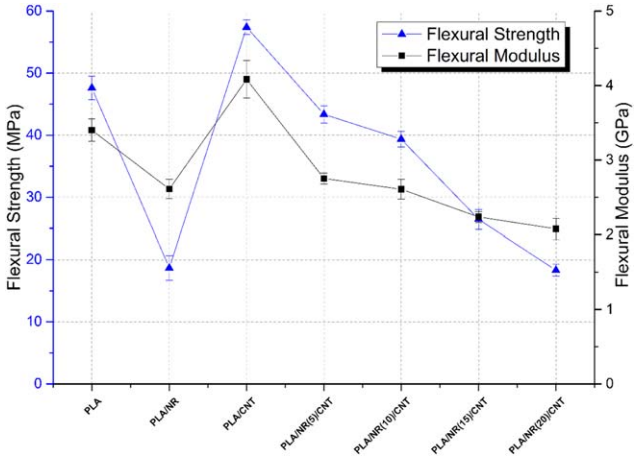

Figure 3. Flexural properties of PLA, PLA/NR, PLA/CNT, and PLA/NR/CNT at various NR contents. [Color figure can be viewed at wileyonlinelibrary.com.]

domains in the PLA matrix. The decrease in flexural properties is similar to the trend displayed in tensile properties observed earlier [Figure 2(a)], thus confirming the dominant role of low-modulus NR in the PLA/NR/CNT nanocomposites. This observation is also supported by other researchers working on NR toughening of PLA/nanoclay nanocomposite systems.[36,40] Interestingly, at low contents of NR, PLA/NR/CNT nanocomposite systems displayed much better stiffness than their PLA/NR/nanoclay counterparts.

The impact test results revealed that NR acted as an efficient impact modifier in the PLA/CNT nanocomposites, illustrated by the increase in impact strength, even at low content of NR. As can be seen from Figure 4, PLA/NR(5)/CNT nanocomposites showed a 124% higher impact strength compared to PLA/CNT nanocomposites. However, it should also be noted that PLA/NR(5)/CNT and PLA/NR(10)/CNT exhibit slightly lower impact strength when compared with PLA/NR. This observation is due to the rigidity of CNT, which decreased the mobility of PLA in the PLA/NR/CNT nanocomposites at lower contents of NR. However,

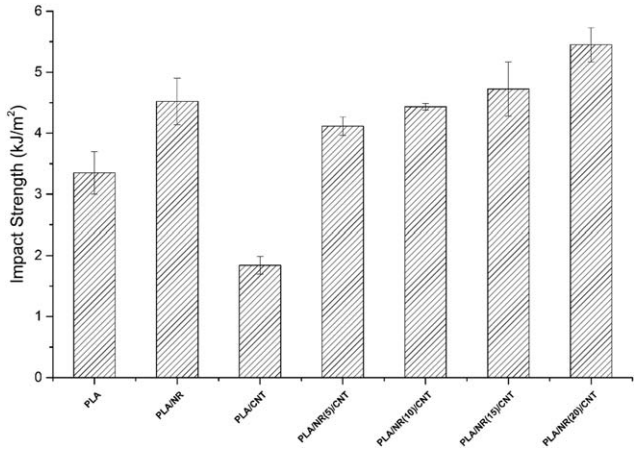

Figure 4. Impact strength of PLA, PLA/NR, PLA/CNT, and PLA/NR/CNT at various NR contents.

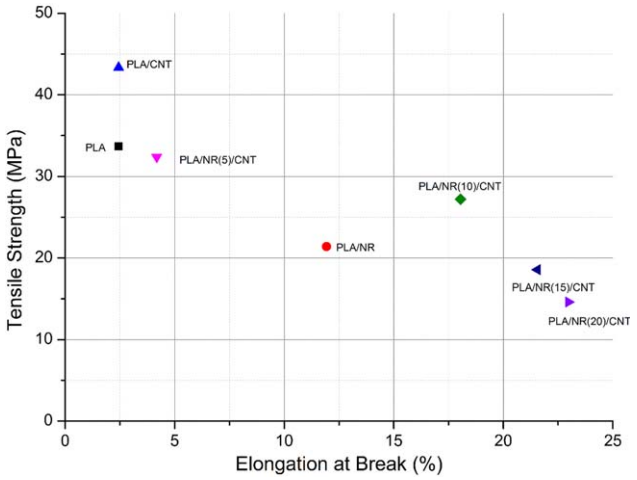

Figure 5. Mechanical properties comparison between PLA, PLA/NR, PLA/CNT, and PLA/NR/CNT based on tensile strength and elongation at break. [Color figure can be viewed at wileyonlinelibrary.com.]

it is worth noting that the impact strength steadily increased with increasing NR content in the ternary nanocomposite blends.

The highest impact strength was observed at PLA/NR/CNT with 20 wt % NR loading, which recorded 21% and 200% increases as compared to PLA/NR and PLA/CNT, respectively. These results are in agreement with previous studies that showed the ability of NR to act as an efficient fracture energy absorber in other nanocomposite systems. In a study by Shi *et al.*[25] on ethylene-*co*-vinyl acetate (EVA) toughened PLA/CNT (PLA/EVA/CNT) nanocomposites, they reported an increase of 192% in impact strength with the incorporation of 20 wt % EVA. Thus, it can be concluded that the NR is an efficient impact modifier comparable to other type of rubbers such as EVA.

The mechanical properties analysis revealed the important finding regarding the trade-off between the improvement in toughness and the decrease in stiffness and tensile strength of NR-toughened PLA/CNT nanocomposite. Figure 5 shows the effect of NR toughening on the tensile strength and elongation at break of NR-toughened PLA/CNT nanocomposites. Tensile strength and elongation at break data of the neat PLA, PLA/NR blend, and PLA/CNT nanocomposite were also included for comparison purposes. It can be observed that PLA/NR(10)/CNT showed the best balance of tensile strength and elongation at break compared to other formulations. As compared to pure PLA and PLA/CNT, this formulation also displayed a significant improvement of elongation at break and at the same time showed the most minimal decrease of elongation at break among all the PLA/NR/CNT nanocomposites.

Morphology

Figure 6 shows the FESEM micrographs of impact fractures in PLA/CNT and PLA/NR/CNT nanocomposites. The morphology of PLA/CNT in Figure 6(a) shows a typical brittle fracture with a rough fracture surface. Generally, all formulations with NR

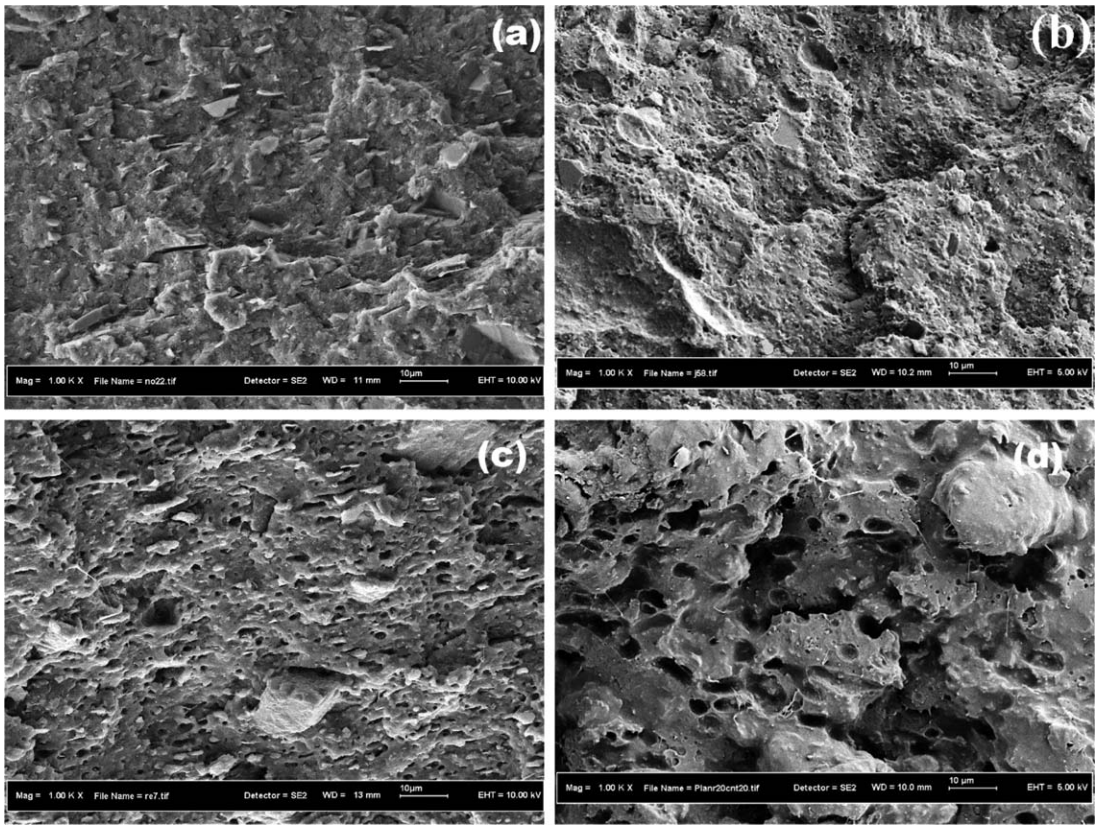

Figure 6. FESEM micrographs taken from impact fracture surfaces at 1000 × magnification of (a) PLA/CNT, (b) PLA/NR(5)/CNT, (c) PLA/NR(10)/CNT, and (d) PLA/NR(20)/CNT.

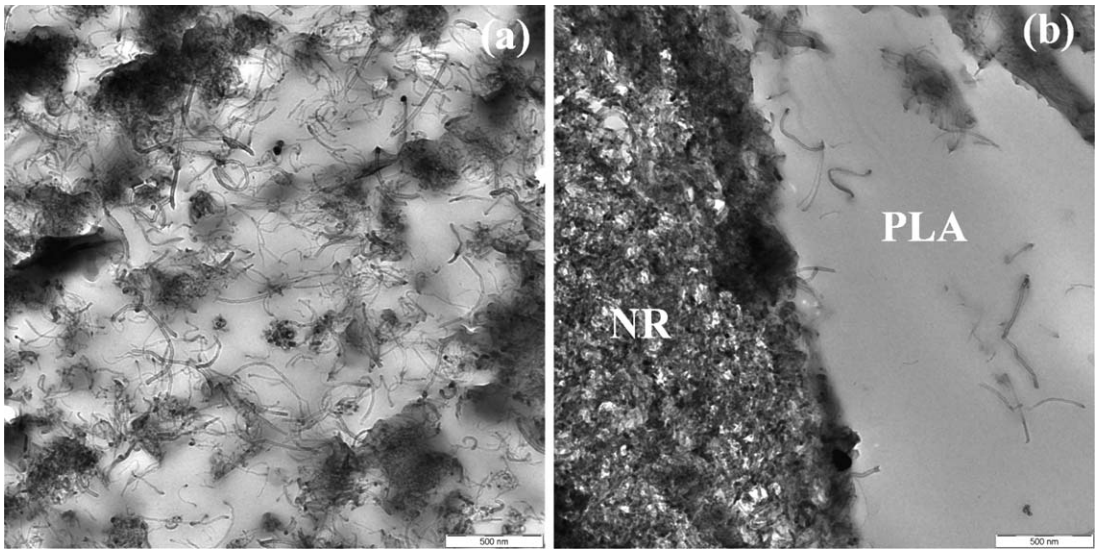

Figure 7. TEM images at 10,000 × magnification of (a) PLA/CNT and (b) PLA/NR/CNT.

show a phase-separated morphology, where the dispersion of rubber particles is distributed in spherical droplets and empty voids throughout the PLA matrix. The spherical-particle-dispersed morphology of rubber in the polymer matrix were also observed by many researchers in an immiscible polymer blend, and this phenomenon was proven to help improve the impact resistance of the brittle PLA by acting as a stress concentrator, initiating and terminating crazes.[26,30] The morphology observation of PLA/NR(5)/CNT nanocomposites shows well-distributed small NR particles and empty voids. Similarly, the morphology of PLA/NR(10)/CNT nanocomposites [Figure 6(c)] also displays a uniform dispersion of NR with slightly larger voids and NR particles. This leads to more resistance to crack propagation and hence enhances the impact properties.[26] On the other hand, the impact fracture surface of PLA/NR(20)/CNT nanocomposites [Figure 6(d)] exhibits the presence of larger empty voids measuring around 5 to 10 μm among the PLA matrix. The existence of such large numbers of empty voids on the surface showed weak interfacial adhesion between NR and the PLA matrix.[39]

TEM observations revealed that PLA/CNT nanocomposites [Figure 7(a)] show a good dispersion of CNTs in the PLA matrix. The PLA/NR/CNT nanocomposites [Figure 7(b)] exhibit the separated phase morphology that is typical for an immiscible blend. Interestingly, in PLA/NR/CNT, the CNTs were found to disperse dominantly in the NR phase rather than in the PLA phase. Therefore, the amount of CNT in the PLA matrix of PLA/NR/CNT nanocomposites was low, which is another possible reason for the decrease in tensile modulus and tensile strength observed earlier. The preference of CNT to not be in the PLA phase was also observed in PLA/EVA/CNT nanocomposites[25] and PLA/poly(butylene adipate-*co*-butylene terephthalate)/CNT nanocomposites.[41] The preferential location of nanofillers in a composite of two different polymers is influenced by interfacial tension and melt viscosity between polymers and the nanofiller.[25] In the case of PLA/NR/CNT nanocomposite systems, the tendency of CNT to reside in the NR phase implies that the interfacial tension of NR-CNT is lower than that of PLA-CNT. It is believed to be caused by Van der Waals interactions between CNT sidewalls and the NR chain, and cation-π bonding between phospholipids at the terminal end of the NR chain with the CNT sidewalls.[42] The higher-magnification TEM image of the PLA/NR/CNT nanocomposite in Figure 8 also reveals interesting observations related to the tendency of CNT to distribute at the interface between PLA and NR (marked in dashed box), which presumably led to better interfacial interaction between NR and PLA. Therefore it can be deduced that CNTs become unifying elements that bind all the components in a PLA/NR/CNT nanocomposite.

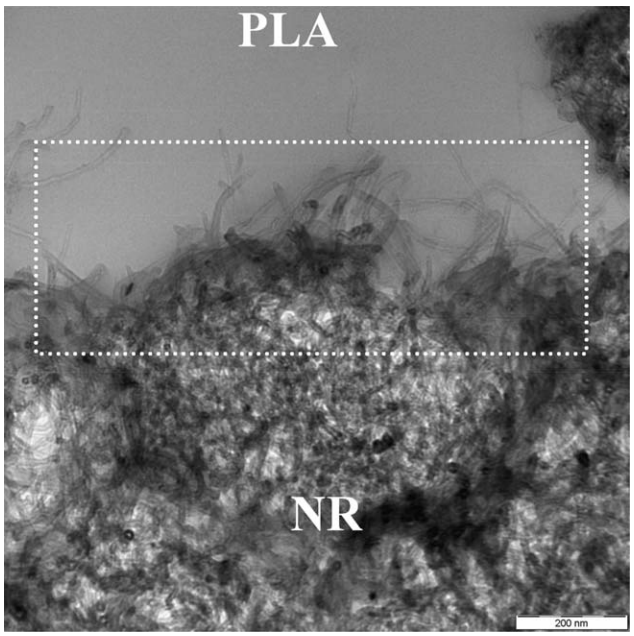

Figure 8. TEM image of PLA/NR/CNT at 25,000 × magnification.

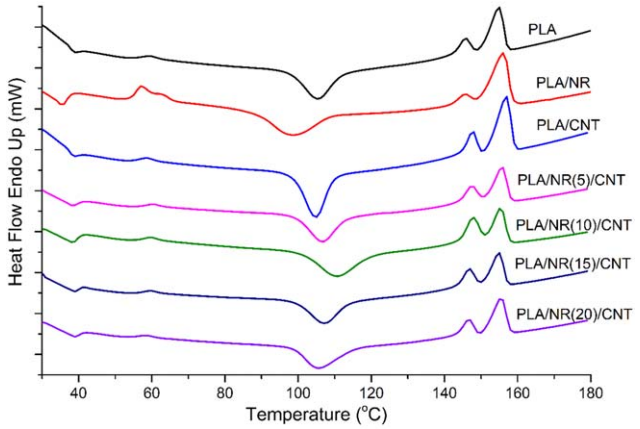

Figure 9. DSC thermograms of second heating run. [Color figure can be viewed at wileyonlinelibrary.com.]

Differential Scanning Calorimetry

DSC thermograms for the second heating cycle of PLA, PLA/NR, PLA/CNT, and PLA/NR/CNT nanocomposites are shown in Figure 9, and the detailed thermal properties are listed in Table III. Two distinct sharp peaks of melting temperature (T_m) were observed in the thermograms of PLA/NR/CNT nanocomposites, which are believed to be caused by the presence of two different PLA crystal structures after the cooling cycle.[43–46] Although no significant changes were observed in the T_m of all the PLA/NR/CNT nanocomposites, the gradual decline of both T_{m1} and T_{m2} with the increase in NR loading is associated with the interference of NR during the formation of the crystalline part of PLA.[39]

On the other hand, DSC analysis also shows that the T_g decreased with the increased content of NR in PLA/CNT nanocomposites. The T_g of PLA/CNT nanocomposites was shifted from 57.2 °C to 55.1 °C for PLA/NR(20)/CNT, so it can be deduced that by having a very low T_g (−70 °C), the presence of NR apparently influenced the reduction of the glass-transition temperature in the PLA/CNT nanocomposite.[30,31] Similar observations were also made in the PLA/NR blends, which showed a reduction of T_g, which was recorded at 53.6 °C as compared to 56.3 °C for the neat PLA. As shown in Figure 9, the DSC thermograms of all the PLA/NR/CNT nanocomposites exhibit the presence of a cold crystallization exothermic peak but at a slightly higher temperature than for the PLA/CNT nanocomposites. Jaratrotkamjorn *et al.*[31] deduced that perhaps NR acted as a nucleating agent, or the molecular weight of the PLA matrix decreased after the blending process, resulting in relatively shorter chains of PLA that can be easily crystallized during heating above the T_g. Furthermore, the presence of CNT, which is widely reported as a good nucleating agent, also contributed to the enhancement of crystallization.[20,25] However, it is also interesting to note that the addition of more rubber into PLA/CNT nanocomposites gradually decreased the crystallinity of the nanocomposites, which might contribute to the drop in the tensile strength and stiffness properties of the PLA/NR/CNT.

Table III. DSC Data for Neat PLA, PLA/NR, PLA/CNT, and PLA/NR/CNT

Formulations	T_g (°C)	T_{m1} (°C)	T_{m2} (°C)	ΔH (J/g)	X_c (%)
PLA	56.3	145.7	154.9	20.4	22.0
PLA/NR	53.6	146.5	155.7	19.46	22.0
PLA/CNT	57.2	147.7	156.9	24.2	28.4
PLA/NR(5)/CNT	57.1	147.4	155.7	19.3	23.0
PLA/NR(10)/CNT	56.2	146.5	155.5	17.5	21.9
PLA/NR(15)/CNT	55.6	147.9	155.4	15.4	20.4
PLA/NR(20)/CNT	55.1	146.7	154.9	14.2	20.0

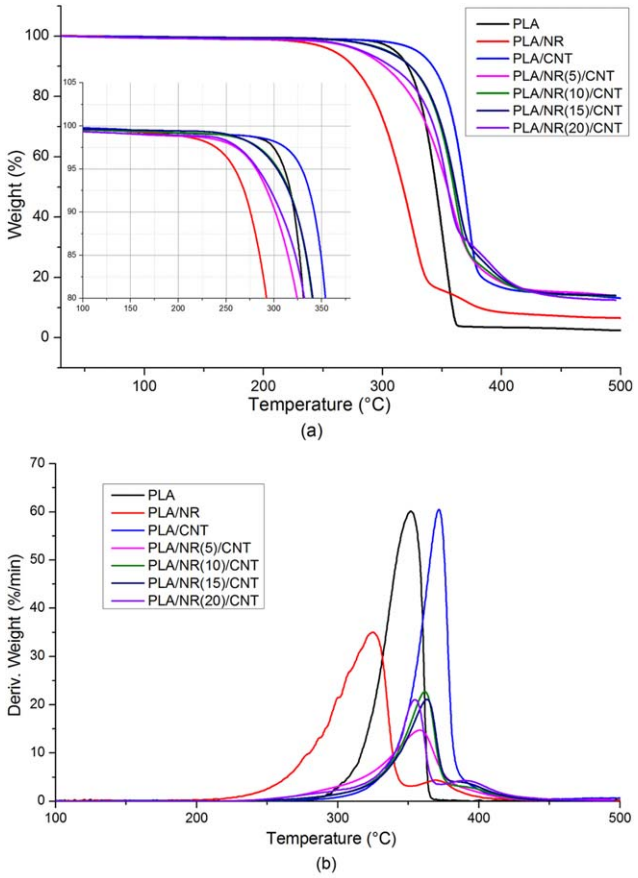

Figure 10. (a) TGA thermograms and (b) DTG curves of PLA, PLA/NR, PLA/CNT, and PLA/NR/CNT nanocomposites. [Color figure can be viewed at wileyonlinelibrary.com.]

Thermal Stability

TGA was performed to investigate the thermal stability of the PLA nanocomposite systems, and the measurements are illustrated as TGA thermogram curves and differential thermal gravimetric (DTG) curves in Figure 10(a) and (b), respectively, and the values of T_{10} and T_{peak} obtained from the analysis are given in Table IV. During early decomposition, the T_{10} shows that the thermal decomposition of all PLA/NR/CNT nanocomposites decreased compared to PLA/CNT nanocomposites. Similarly, a significant decrease was observed in T_{peak} values for all PLA/NR/CNT nanocomposites compared to T_{peak} for PLA/CNT nanocomposites. The most drastic decline of T_{peak} was observed

Table IV. Thermal Degradation Values for PLA, PLA/NR, PLA/CNT, and PLA/NR/CNT

Formulations	T_{10} (°C)	T_{peak} (°C)
PLA	321.3	352.0
PLA/NR	275.5	325.0
PLA/CNT	342.3	371.6
PLA/NR(5)/CNT	301.6	358.1
PLA/NR(10)/CNT	323.5	361.7
PLA/NR(15)/CNT	323.4	363.1
PLA/NR(20)/CNT	307.1	354.6

for PLA/NR(20)/CNT nanocomposites, which was recorded at 301.1 °C, as opposed to 354.6 °C for the PLA/CNT nanocomposites. Based on these findings, it can be concluded that the addition of NR significantly decreased the thermal stability of PLA/CNT nanocomposites. The PLA/NR/CNT nanocomposites with 10 and 15 wt % NR recorded almost similar values of T_{10} and T_{peak} and were also the most thermally stable nanocomposites among the studied PLA/NR/CNT formulations. As can be observed from Figure 10, PLA/NR/CNT nanocomposites generally showed higher thermal stabilities compared to the PLA/NR blend and neat PLA. The improvement in the thermal stabilities of nanocomposites is due to the uniform dispersion of CNT nanofillers in the PLA matrix, as confirmed earlier by the TEM results. The uniform dispersion of CNT nanofillers retarded the diffusion of oxygen into the polymer matrix through tortuous paths and barrier effects against the volatile pyrolized products of PLA, eventually retarding the thermal degradation of the polymer nanocomposites.[47]

CONCLUSIONS

A PLA/NR blend and PLA/CNT and PLA/NR/CNT nanocomposites were prepared by a melt-blending method using a counterrotating twin-screw extruder. The PLA/NR blend exhibited significant increases in impact strength and elongation at break compared to neat PLA (approximately 35% and 400%, respectively). The tensile strength and Young's modulus of PLA/CNT nanocomposites were increased approximately 29% and 4% by the incorporation of CNTs, respectively. In addition, the flexural strength, flexural modulus, and thermal stability of PLA/CNT increased, whereas the impact strength decreased compared to neat PLA. The toughness of PLA/CNT was improved significantly by the incorporation of NR. The highest impact strength and elongation at break of PLA/NR/CNT was observed at 20 wt % NR content, which showed approximately 200% and 840% increases compared to PLA/CNT nanocomposites, respectively. However, the tensile strength, tensile modulus, and flexural properties of PLA/CNT decreased with the addition of NR. Based on the mechanical testing of the obtained nanocomposites, the PLA/NR(10)/CNT nanocomposite can be suggested as an optimum formulation with balanced mechanical properties compared to other formulations. FESEM and TEM analyses revealed that the NR particles are homogeneously dispersed in PLA/NR/CNT nanocomposites, while the CNTs preferentially reside in the NR phase rather than in the PLA matrix. The TGA analysis showed that the addition of NR into PLA/CNT nanocomposites decreased the thermal stability of the nanocomposites. In addition, PLA/NR/CNT exhibited a lower T_g and degree of crystallinity than neat PLA/CNT nanocomposites.

ACKNOWLEDGMENTS

The authors wish to acknowledge the Ministry of Education Malaysia, Universiti Teknologi Malaysia for financial support of this research (grant no. 03H08), Universiti Malaysia Pahang, Idemitsu-PS (M) Sdn. Bhd. for permitting the use of the Toyoseiki impact tester, and the Malaysia Rubber Board for the donation of natural rubber.

REFERENCES

1. Ray, S. S.; Okamoto, M. *Macromol. Rapid Commun.* **2003**, *24*, 815.
2. Anderson, K. S.; Schreck, K. M.; Hillmyer, M. A. *Polym. Rev.* **2008**, *48*, 85.
3. Jamshidian, M.; Tehrany, E. A.; Imran, M.; Jacquot, M.; Desobry, S. *Compr. Rev. Food Sci. Food Safety* **2010**, *9*, 552.
4. Liu, H.; Zhang, J. *J. Polym. Sci., Part B: Polym. Phys.* **2011**, *49*, 1051.
5. Balakrishnan, H.; Hassan, A.; Imran, M.; Wahit, M. U. *Polym.-Plast. Technol. Eng.* **2012**, *51*, 175.
6. Li, T.; Turng, L.-S.; Gong, S.; Erlacher, K. *Polym. Eng. Sci.* **2006**, *46*, 1419.
7. Moon, S.-I.; Jin, F.; Lee, C.-J.; Tsutsumi, S.; Hyon, S.-H. *Macromol. Symp.* **2005**, *224*, 287.
8. Wu, C.-S.; Liao, H.-T. *Polymer* **2007**, *48*, 4449.
9. Chiu, W.-M.; Chang, Y.-A.; Kuo, H.-Y.; Lin, M.-H.; Wen, H.-C. *J. Appl. Polym. Sci.* **2008**, *108*, 3024.
10. Bourbigot, S.; Fontaine, G.; Gallos, A.; Bellayer, S. *Polym. Adv. Technol.* **2011**, *22*, 30.
11. Ramontja, J.; Ray, S. S.; Pillai, S. K.; Luyt, A. S. *Macromol. Mater. Eng.* **2009**, *294*, 839.
12. Mat Desa, M. S. Z.; Hassan, A.; Arsad, A.; Mohammad, N. N. B. *Mater. Res. Innovations* **2014**, *18*, 14.
13. Kim, I.-H.; Jeong, Y. G. *J. Polym. Sci., Part B: Polym. Phys.* **2010**, *48*, 850
14. Jiang, L.; Zhang, J.; Wolcott, M. P. *Polymer* **2007**, *48*, 7632.
15. Petersson, L.; Oksman, K. *Compos. Sci. Technol.* **2006**, *66*, 2187.
16. Murariu, M.; Dechief, A.-L.; Paint, Y.; Peeterbroeck, S.; Bonnaud, L.; Dubois, P. *J. Polym. Environ.* **2012**, *20*, 932.
17. Krul, L. P.; Volozhyn, A. I.; Belov, D. A.; Poloiko, N. A.; Artushkevich, A. S.; Zhdanok, S. A.; Solntsev, A. P; Krauklis, A. V.; Zhukova, I. A. *Biomol. Eng.* **2007**, *24*, 93.
18. Tsuji, H.; Kawashima, Y.; Takikawa, H.; Tanaka, S. *Polymer* **2007**, *48*, 4213.
19. Pilla, S.; Kramschuster, A; Gong, S; Chandra, A; Turng, L. S. *Int. Polym. Process.* **2007**, *22*, 418.
20. Villmow, T.; Pötschke, P.; Pegel, S.; Häussler, L.; Kretzschmar, B. *Polymer* **2008**, *49*, 3500.

21. Lemmouchi, Y.; Murariu, M.; Santos, A. M. D.; Amass, A. J.; Schacht, E.; Dubois, P. *Eur. Polym. J.* **2009**, *45*, 2839.
22. Anderson, K. S.; Hillmyer, M. A. *Polymer* **2004**, *45*, 8809.
23. Anderson, K. S.; Lim, S. H.; Hillmyer, M. A. *J. Appl. Polym. Sci.* **2003**, *89*, 3757.
24. Vilay, V.; Mariatti, M.; Ahmad, Z.; Pasomsouk, K.; Todo, M. *J. Appl. Polym. Sci.* **2009**, *114*, 1784.
25. Shi, Y.; Li, Y.; Wu, J.; Huang, T.; Chen, C.; Peng, Y.; Wang, Y. *J. Polym. Sci., Part B: Polym. Phys.* **2011**, *49*, 267.
26. Ishida, S.; Nagasaki, R.; Chino, K.; Dong, T.; Inoue, Y. *J. Appl. Polym. Sci.* **2009**, *113*, 558.
27. Juntuek, P.; Ruksakulpiwat, C.; Chumsamrong, P.; Ruksakulpiwat, Y. *Adv. Mater. Res.* **2010**, *123*, 1167.
28. Bitinis, N.; Verdejo, R.; Cassagnau, P.; Lopez-Manchado, M. A. *Mater. Chem. Phys.* **2011**, *129*, 823.
29. Nampitch, T.; Magaraphan, R. *Adv. Mater. Res.* **2011**, *335*, 762.
30. Zhang, C.; Man, C.; Pan, Y.; Wang, W.; Jiang, L.; Dan, Y. *Polym. Int.* **2011**, *60*, 1548.
31. Jaratrotkamjorn, R.; Khaokong, C.; Tanrattanakul, V. *J. Appl. Polym. Sci.* **2012**, *124*, 5027.
32. Juntuek, P.; Ruksakulpiwat, C.; Chumsamrong, P.; Ruksakulpiwat, Y. *J. Appl. Polym. Sci.* **2012**, *125*, 745.
33. Phruksaphithak, N.; Noomhorm, C. *Adv. Mater. Res.* **2012**, *486*, 406.
34. Chuayjuljit, S.; Moolsin, S.; Potiyaraj, P. *J. Appl. Polym. Sci.* **2005**, *95*, 826.
35. Mohammad, N. N. B; Arsad, A.; Rahmat, A. R.; Sani, A. S. *Mater. Sci. Forum* **2015**, *819*, 284.
36. Bijarimi, M.; Ahmad, S.; Rasid, R. *J. Elast. Plast.* **2014**, *46*, 338.
37. Mat Desa, M. S. Z.; Hassan, A.; Arsad, A. *Adv. Mater. Res.* **2013**, *747*, 639.
38. Mohammad, N. N. B.; Arsad, A.; Rahmat, A. R.; Mat Desa, M. S. Z.; Sani, A. S. *Appl. Mech. Mater.* **2014**, *695*, 273.
39. Pongtanayut, K.; Thongpin, C.; Santawitee, O. *Energy Procedia* **2013**, *34*, 888.
40. Bitinis, N.; Verdejo, R.; Maya, E. M.; Espuche, E.; Cassagnau, P.; Lopez-Manchado, M. A. *Compos. Sci. Technol.* **2012**, *72*, 305.
41. Ko, S.; Hong, M.; Park, B.; Gupta, R.; Choi, H.; Bhattacharya, S. *Polym. Bull.* **2009**, *63*, 125.
42. Le, H. H.; Abhijeet, S.; Ilisch, S.; Klehm, J.; Henning, S.; Beiner, M.; Sarkawi, S. S.; Dierkes, W.; Das, A.; Fischer, D.; Stöckelhuber, K.-W.; Wiessner, S.; Khatiwada, S. P.; Adhikari, R.; Pham, T.; Heinrich, G.; Radusch, H.-J. *Polymer* **2014**, *55*, 4738.
43. Mina, M. F.; Beg, M. D. H.; Islam, M. R.; Nizam, A.; Alam, A. K. M. M.; Yunus, R. M. *Polym. Eng. Sci.* **2014**, *54*, 317.
44. Yasuniwa, M.; Tsubakihara, S.; Sugimoto, Y.; Nakafuku, C. *J. Polym. Sci., Part B: Polym. Phys.* **2004**, *42*, 25.
45. Di Lorenzo, M. L. *Macromol. Symp.* **2006**, *234*, 176.
46. Pan, P.; Kai, W.; Zhu, B.; Dong, T.; Inoue, Y. *Macromolecules* **2007**, *40*, 6898.
47. Arjmandi, R.; Hassan, A.; Haafiz, M. K. M.; Zakaria, Z.; Islam, M. S. *Int. J. Biol. Macromol.* **2016**, *82*, 998.